Supporting Information

Rapid One-pot Microwave-assisted Synthesis and Defect Engineering of UiO-66 for Enhanced CO_2 Capture

Dong A. Kang[a], Amro M. O. Mohamed[c] Christian Murphy[a], Andres Ramos[a], Ioannis G. Economou[c], Jinsoo Kim[d], and Hae-Kwon Jeong[*,a,b,d]

[a]Artie McFerrin Department of Chemical Engineering and [b]Department of Materials Science and Engineering, Texas A&M University, 3122 TAMU, College Station, TX 77843-3122, United States

[c]Chemical Engineering Program, Texas A&M University at Qatar, PO Box 23874, Doha, Qatar

[d]Department of Chemical Engineering (Integrated Engineering), Kyung Hee University, 1732 Deogyeong-daero, Yongin, Gyeonggi-do 17104, Republic of Korea

** Corresponding author*

H.-K. Jeong (e-mail address: hjeong7@tamu.edu, Phone: +1-979-862-4850, Fax: +1-979-845-6446)

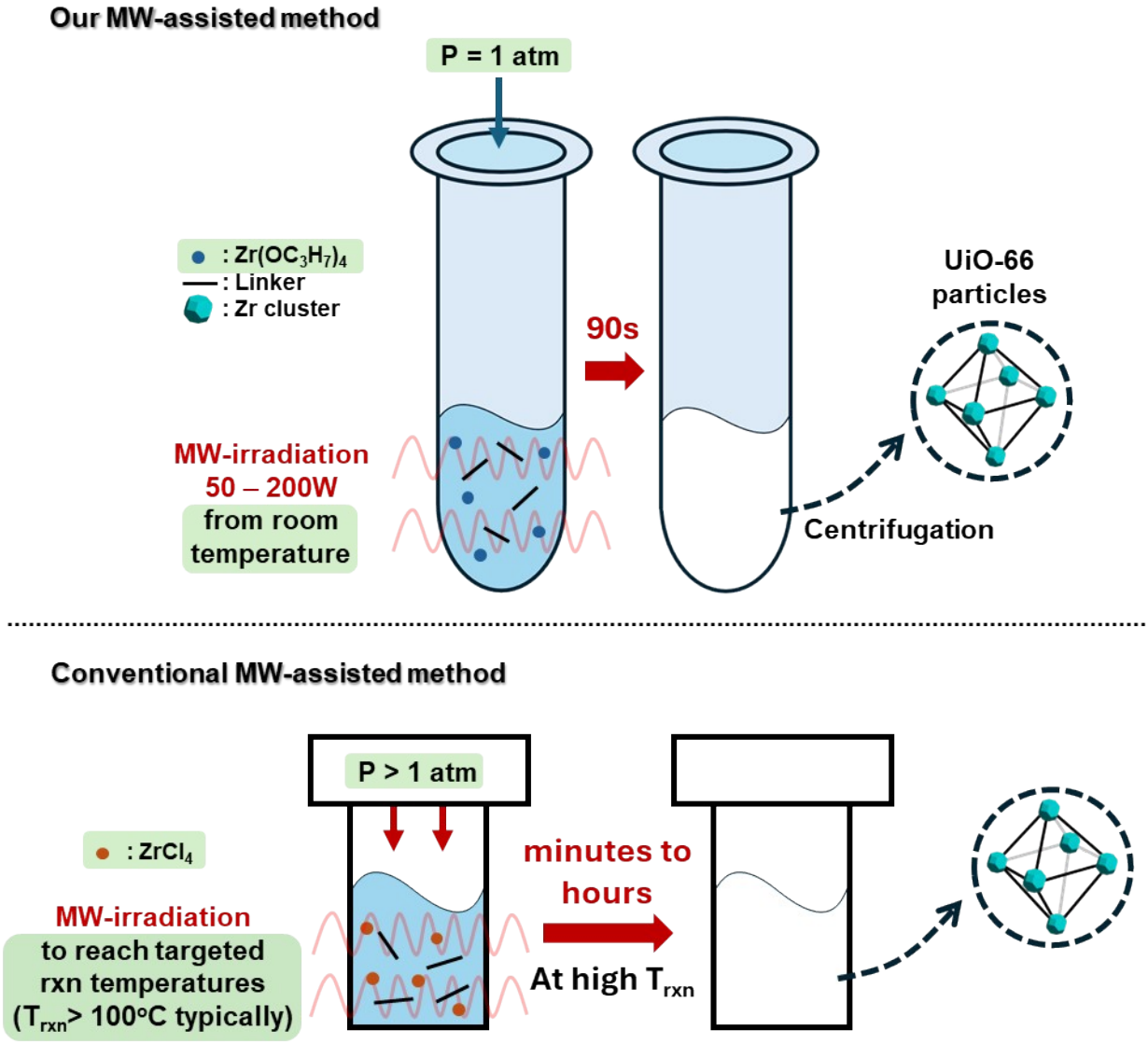

Figure S1 Schematic illustration of our one-pot rapid MW-assisted synthesis compared to conventional MW-assisted synthesis methods (i.e., autogenous temperature vs. autogenous pressure).

Table S1. Comparison of MW-assisted synthesis methods for UiO-66 with literature.

Metal precursor	Radiation power (W)	Radiation time (mins)	Reaction temperature (°C)	Pressure (atm)	BET surface area (m^2/g)	Yield (%)	Ref.
$Zr(OC_3H_7)_4$	50 – 200W	1.5	-	1	~ 1731	25 - 64	This work
$ZrCl_4$	80 → 200 (two step)	18	-	> 1 (autogenous)	~ 1206	78	[1]
	-	92	180		~ 1789	-	[2]
	350	5 - 30	80 – 120		~ 1320	45 – 91	[3]
	130	3	110		-	88	[4]
	-	120	100		~ 1661	80 – 90	[5]
	-	360	80		~ 318	-	[6]

Table S2. Detailed conditions of precursor solutions for synthesizing UiO-66.

70wt% $Zr(OC_3H_7)_4$ solution	**Zr**	**Linker**	**DMF**	**Acetic acid**
0.60 g	1.28 mmol	TA, 0.20g (1.20 mmol)	28 ml (440 mmol)	16 ml (230 mmol)

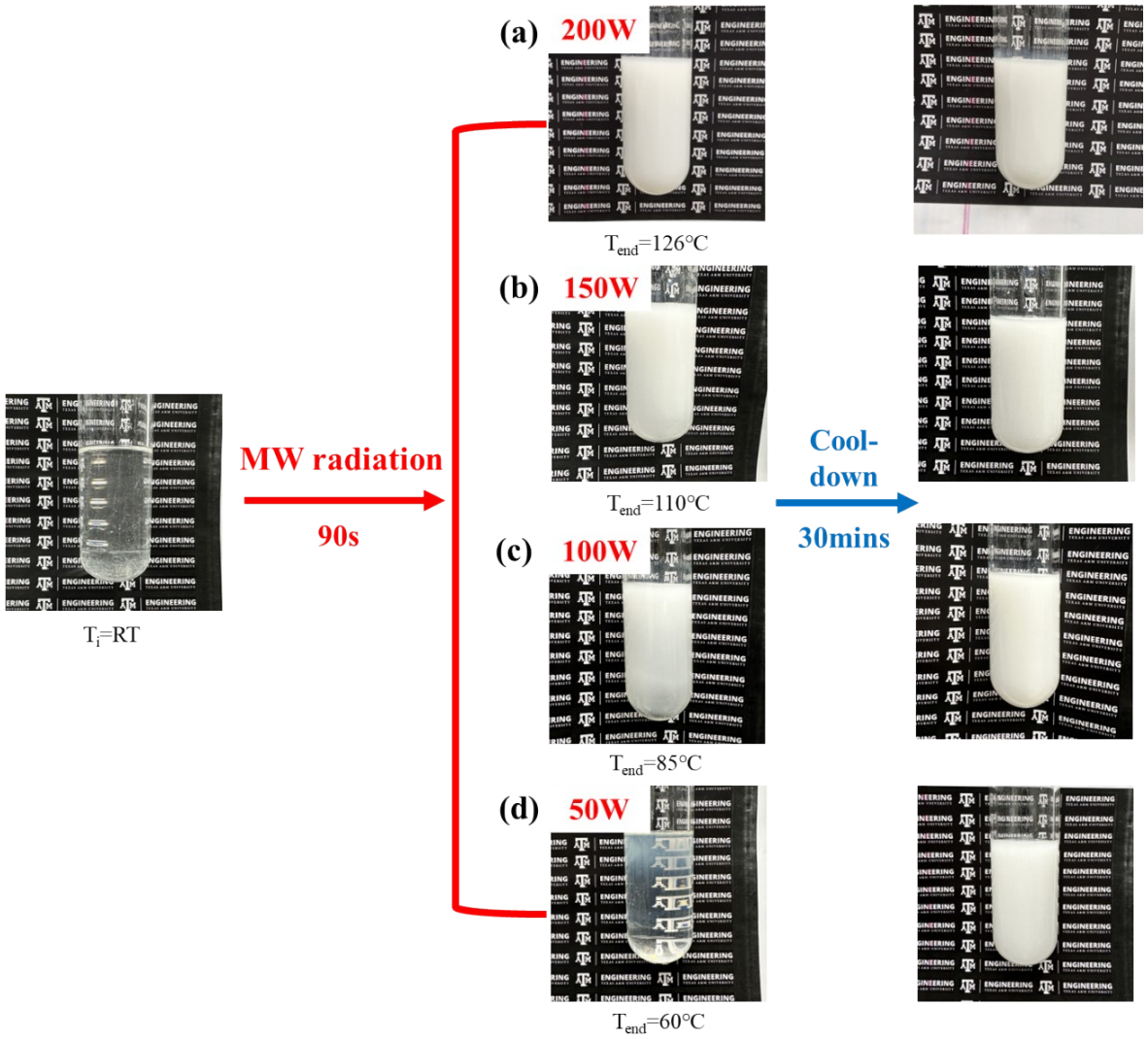

Figure S2 Photographs of the synthesis process for UiO-66 under microwave irradiation (T_i: temperature before MW radiation and T_{end}: temperature after MW radiation).

Figure S3 Photographs of UiO-66 synthesis solutions: **(a)** before MW radiation and **(b)** after MW radiation at 200 W.

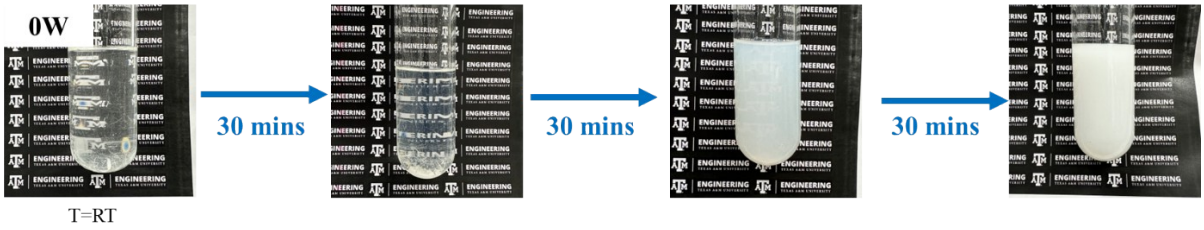

Figure S4 Photographs of time-dependent UiO-66 synthesis solution without MW radiation.

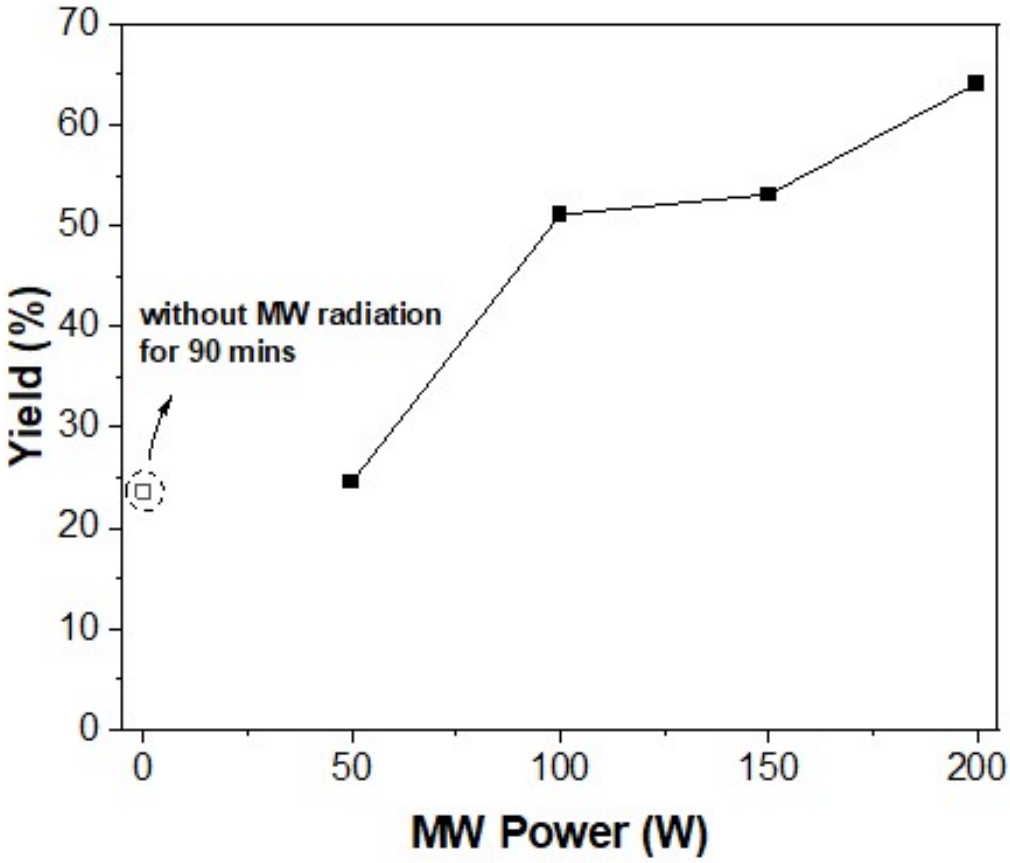

Figure S5 Synthesis yields of MW-assisted synthesized UiO-66 in this work.

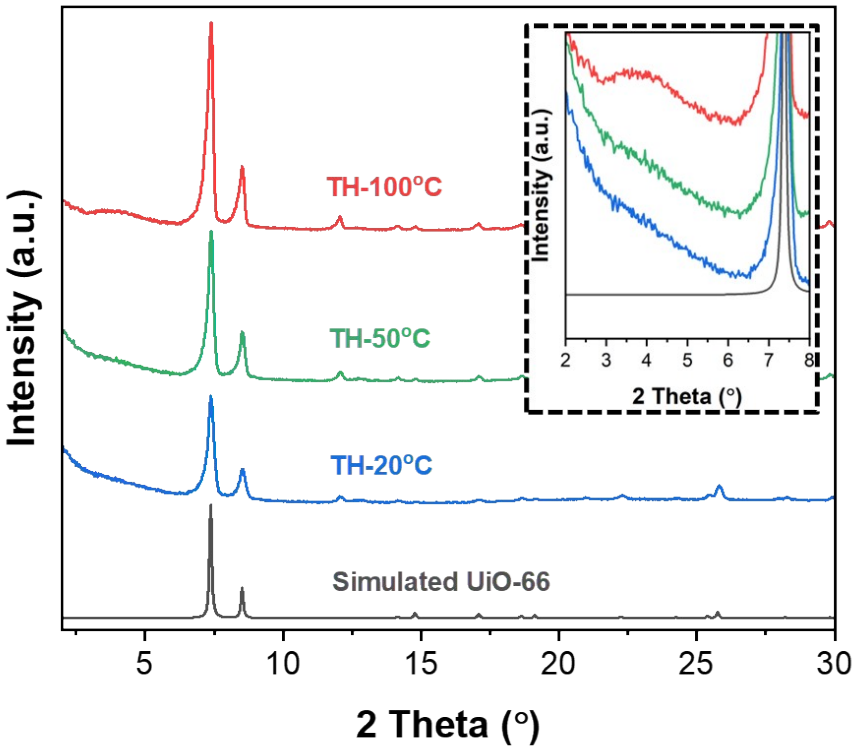

Figure S6 PXRD patterns of UiO-66 synthesized by the thermal method at different synthesis temperatures.

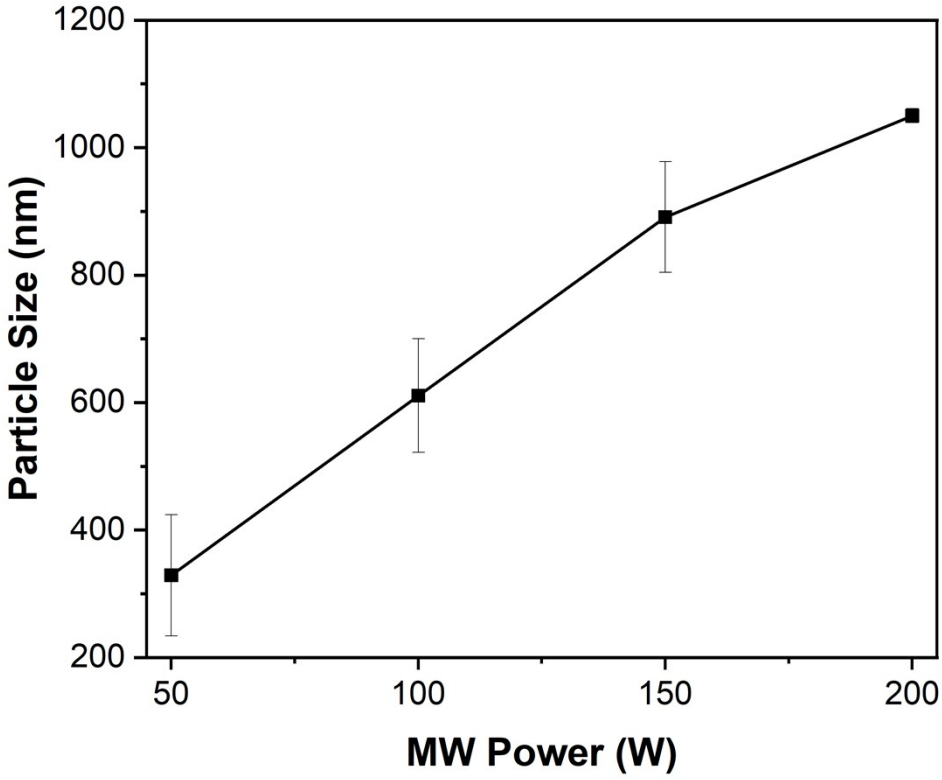

Figure S7 Particle size of UiO-66 synthesized as a function of MW power.

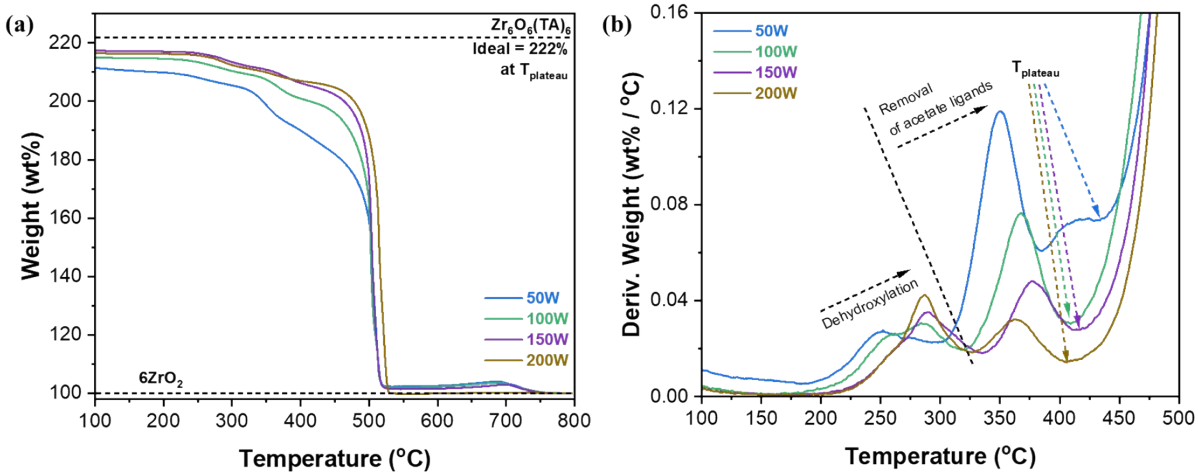

(c)

1. At $T_{plateau}$, the sample is assumed to be $Zr_6O_{6+x}(TA)_{6-x}$ (ideal: $Zr_6O_6(TA)_6$) after desolvation (25-100°C), dehydroxylation (200-325°C), and removal of acetate ligand (~390°C) occur (Hence, x presents linker deficiencies per Zr_6 unit (i.e., defectivity))
2. A very large weight loss over a temperature range of ca. 390-525 °C due to the collapse of the MOF framework (via combustion of the TA linkers).
3. At 800°C, the sample is assumed to become fully decomposed into $6ZrO_2$
4. Based on the assumptions above,

$$Wt_{plateau} = \frac{MW_{Zr_6O_{6+x}(linker)_{6-x}}}{6 \times MW_{ZrO_2}} \times 100$$

where, MW_x presents the molecular weight of species x, and $Wt_{plateau}$ presents the normalized weight percent of a sample at $T_{plateau}$, relative to the mass of ZrO_2 in the TGA results.

Figure S8 (a) TGA and **(b)** DTG curves of UiO-66 synthesized at varying MW-radiation power, and **(c)** a method to calculate linker deficiencies per Zr_6 unit (defectivity).

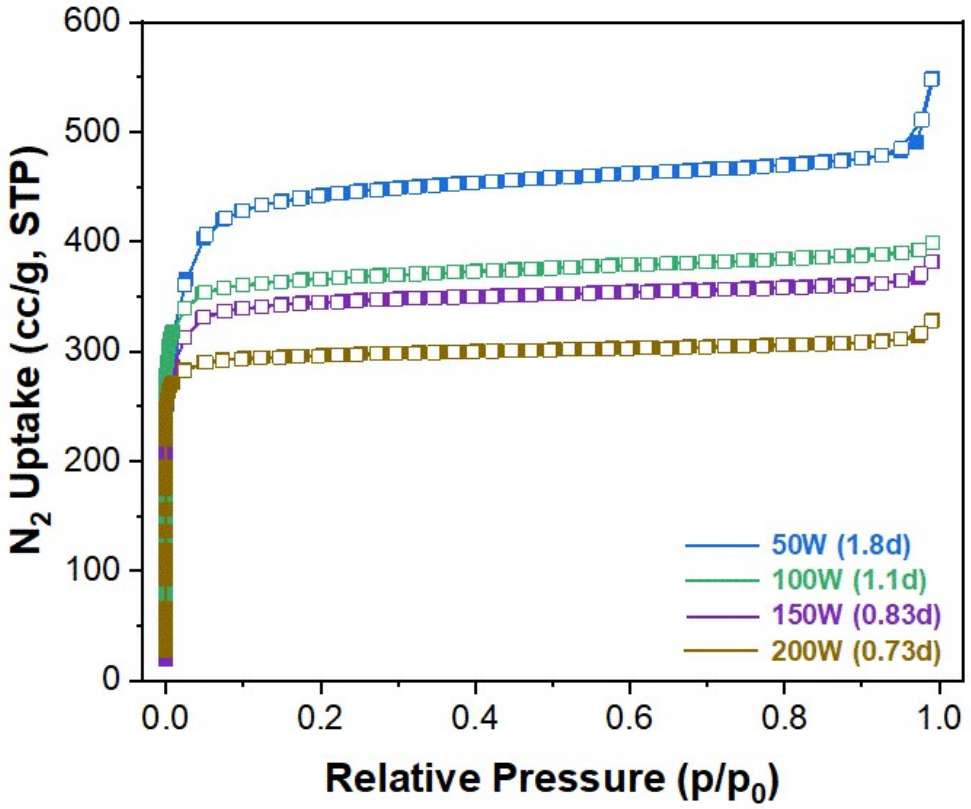

Figure S9 N_2 isotherms at 77K of UiO-66 synthesized at varying MW-radiation power.

Table S3. Textural properties of UiO-66 synthesized at varying MW-radiation power**.**

MW Power	Defectivity (d)	S_{BET} (m^2/g)	V_{mic} (cm^3/g)	V_t (cm^3/g)
50 W	1.8	1731	0.638	0.850
100 W	1.1	1419	0.538	0.618
150 W	0.83	1344	0.517	0.592
200 W	0.73	1148	0.444	0.508

(S_{BET}: BET surface area, V_{mic}: micropore volume, V_t: total pore volume). Defectivity (d) is defined as linker deficiencies per Zr_6 unit (see Fig. S7))

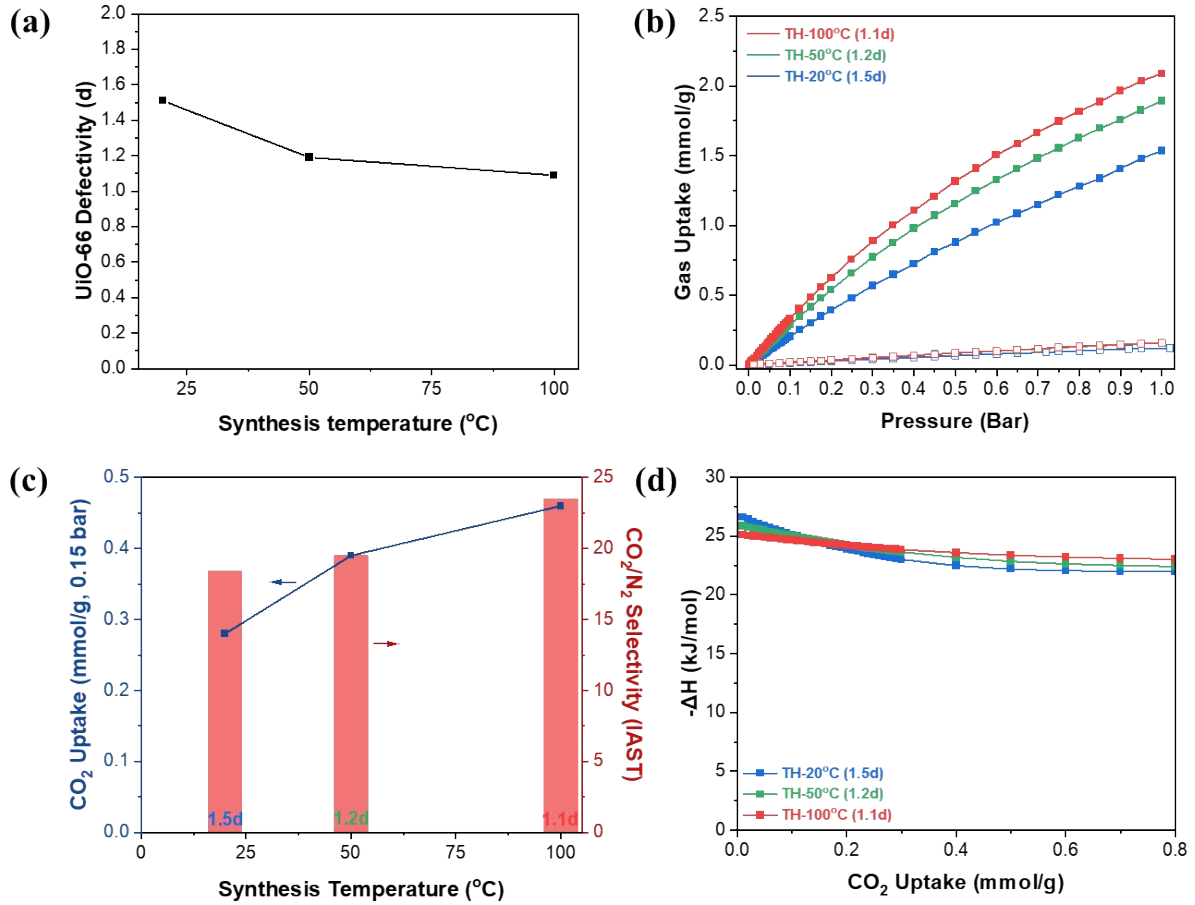

Figure S10 (a) Defectivity (d) of thermally (TH)-synthesized UiO-66 as a function of synthesis temperature, **(b)** CO_2 and N_2 pure gas isotherms at 30°C of UiO-66 synthesized by the TH method at varying synthesis temperature, **(c)** IAST CO_2 uptake at 0.15 bar and CO_2/N_2 selectivity as a function of synthesis temperature (line: CO_2 uptake (left axis), bar: CO_2/N_2 selectivity (right axis)), and **(d)** CO_2 isosteric heat of adsorption of UiO-66 by the TH method at varying synthesis temperature.

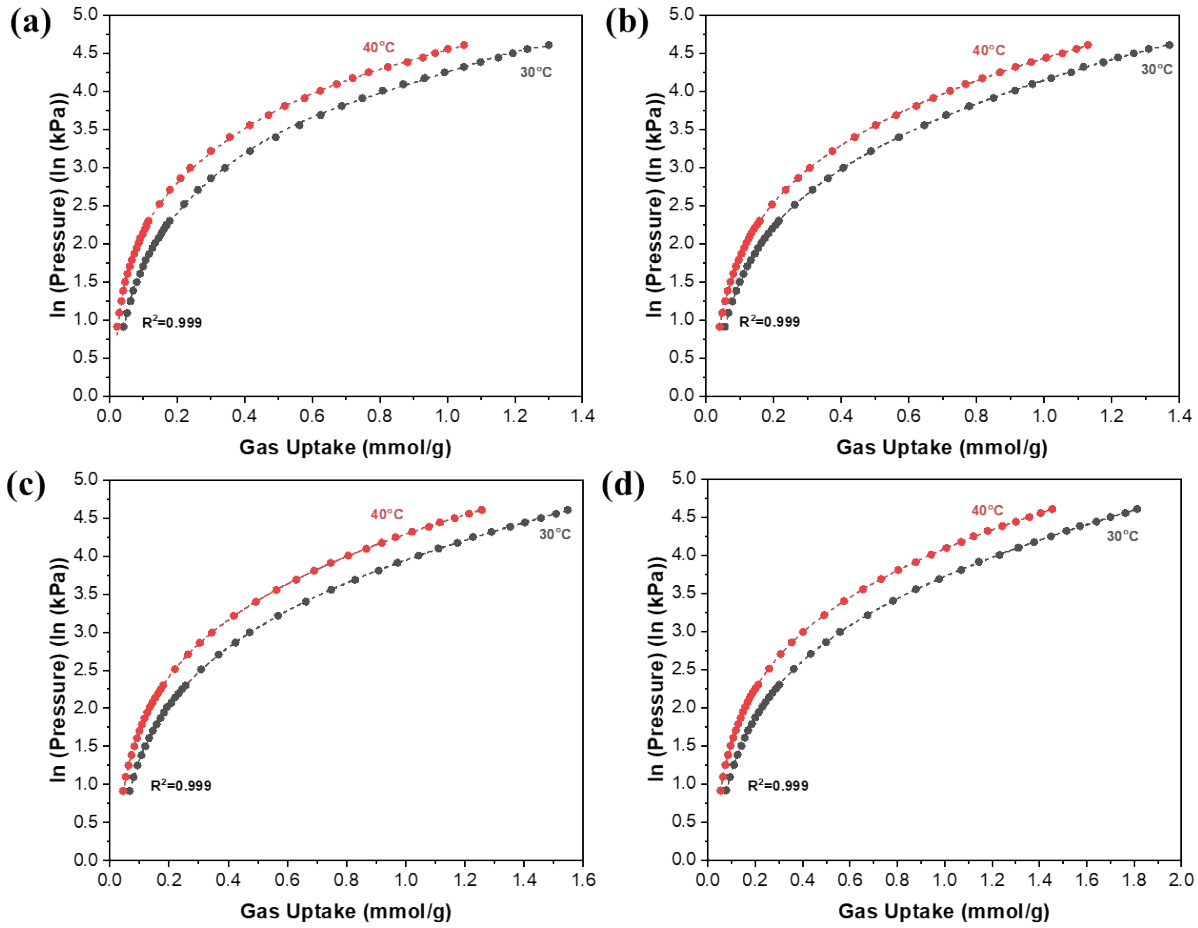

Figure S11 CO_2 adsorption isotherms of UiO-66 synthesized at varying MW power at 30 and 40°C and their fits with virial equations: **(a)** 50 W, **(b)** 100 W, **(c)** 150 W and **(d)** 200 W (points: experimental, dashed lines: virial fitting).

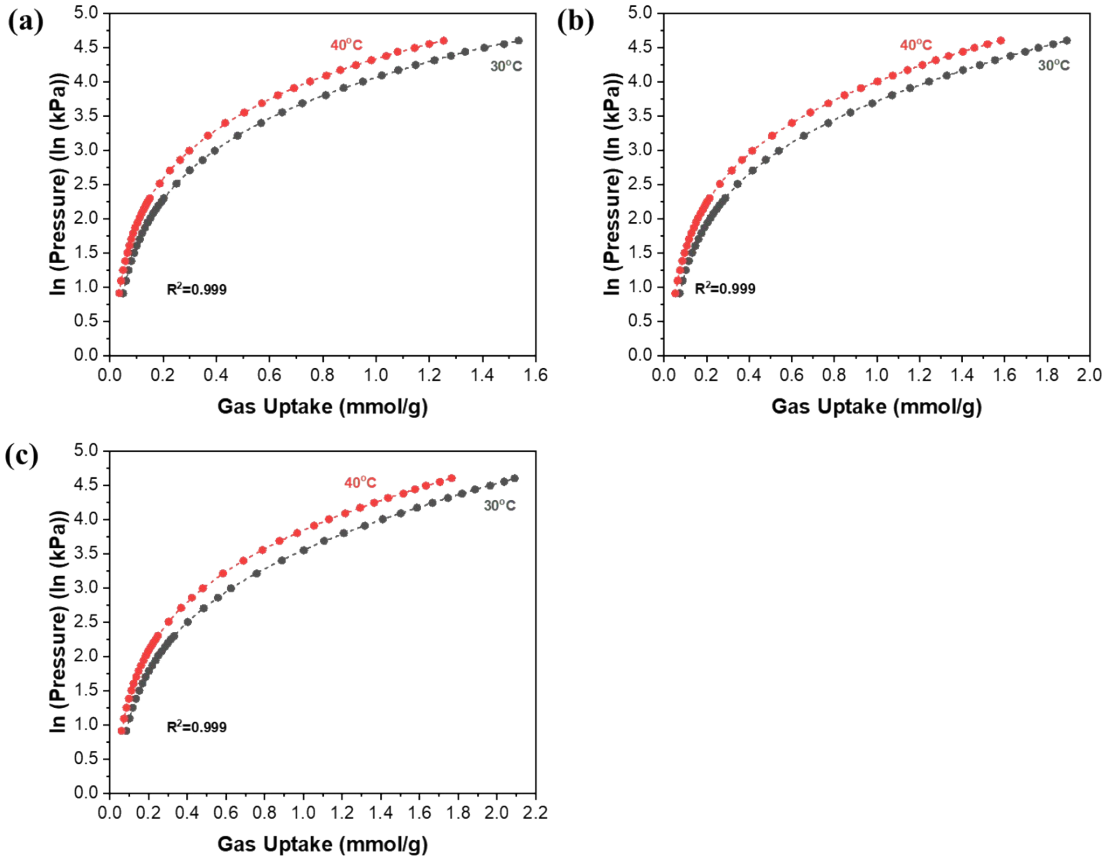

Figure S12 CO_2 adsorption isotherms of UiO-66 by the TH method at varying synthesis temperature at 30 and 40℃ and their fits with virial equations: **(a)** 20 ºC **(b)** 50 ºC and **(c)** 100 ºC (points: experimental, dashed lines: virial fitting).

Table S4. Comparison of CO_2 capacity and CO_2/N_2 selectivity of UiO-66 with those in literatures.

Synthesis method	CO_2 capacity (at 0.15 bar, mmol/g)	CO_2/N_2 selectivity (ideal)	CO_2/N_2 selectivity (IAST)	Temperature (^oC)	Ref
MW-assisted	0.26	24.5	41[a]	30	This work
Solvothermal	0.55	-	22.8[a]	25	[7]
	0.50	-	20[b]	25	[8]
	0.40	18	-	25	[9]
	0.44	-	25[b]	25	[10]

([a]: at 0.15 bar CO_2 / 0.85 bar N_2 and [b]: at 0.5 bar CO_2 / 0.5 bar N_2)

Table S5. Computational largest cavity parameter (LCD) and pore limiting diameter (LPD) for pristine UiO-66 and defective structures. The three values in each in LCD and PLD in every row provide the values for each crystallographic direction.

Linker deficiency (per Zr_6 node)	**LCD (Å)**			**PLD (Å)**		
0	8.452			3.785		
0.25	8.550	8.413	8.432	3.785	3.790	3.791
0.5	8.550	8.432	8.432	3.785	3.840	4.900
0.75	8.550	8.430	8.432	6.253	3.840	4.900
1	8.550	8.432	8.432	6.253	3.840	4.899
1.25	8.550	8.432	8.432	6.681	3.840	4.928
1.5	8.550	8.432	8.433	6.952	3.840	4.786
1.75	8.550	8.432	8.428	6.952	3.840	4.874
2	8.550	8.432	8.408	6.952	3.842	5.191

References

1. M. Taddei, P. V. Dau, S. M. Cohen, M. Ranocchiari, J. A. van Bokhoven, F. Costantino, S. Sabatini and R. Vivani, *Dalton transactions*, 2015, **44**, 14019-14026.
2. W. Liang, C. J. Coghlan, F. Ragon, M. Rubio-Martinez, D. M. D'Alessandro and R. Babarao, *Dalton Transactions*, 2016, **45**, 4496-4500.
3. T. K. Vo, V. N. Le, K. S. Yoo, M. Song, D. Kim and J. Kim, *Crystal Growth & Design*, 2019, **19**, 4949-4956.
4. L. H. T. Nguyen, T. T. T. Nguyen, Y. T. Dang, P. H. Tran and T. Le Hoang Doan, *Asian Journal of Organic Chemistry*, 2019, **8**, 2276-2281.
5. Y. Li, Y. Liu, W. Gao, L. Zhang, W. Liu, J. Lu, Z. Wang and Y.-J. Deng, *CrystEngComm*, 2014, **16**, 7037-7042.
6. M. Yahia, L. A. Lozano, J. M. Zamaro, C. Téllez and J. Coronas, *Separation and Purification Technology*, 2024, **330**, 125558.
7. G. E. Cmarik, M. Kim, S. M. Cohen and K. S. Walton, *Langmuir*, 2012, **28**, 15606-15613.
8. N. C. Pham, T. K. Vo, Q. B. Nguyen, T. K. Nguyen, T. H. C. Nguyen, N. N. Dao, J. Kim and V. C. Nguyen, *Inorganic Chemistry Communications*, 2023, **158**, 111476.
9. A. Huang, L. Wan and J. Caro, *Materials Research Bulletin*, 2018, **98**, 308-313.
10. J. Yan, T. Ji, Y. Sun, S. Meng, C. Wang and Y. Liu, *Journal of Membrane Science*, 2022, **661**, 120959.